J Neurophysiol 99: 1294–1305, 2008.
First published January 23, 2008; doi:10.1152/jn.01191.2007.

Effects of Striatal $GABA_A$-Receptor Blockade on Striatal and Cortical Activity in Monkeys

Olivier Darbin[1] and Thomas Wichmann[1,2]

[1]*Division of Sensorimotor Systems, Yerkes National Primate Center and* [2]*Department of Neurology, Emory University, Atlanta, Georgia*

Submitted 25 October 2007; accepted in final form 18 January 2008

Darbin O, Wichmann T. Effects of striatal $GABA_A$-receptor blockade on striatal and cortical activity in monkeys. *J Neurophysiol* 99: 1294–1305, 2008. First published January 23, 2008; doi:10.1152/jn.01191.2007. To elucidate the role of ambient striatal γ-aminobutyric acid (GABA) in the regulation of neuronal activity in the basal ganglia–thalamocortical circuits, we studied the effects of blocking striatal $GABA_A$ receptors on the electrical activities of single striatal neurons, on local field potentials (LFPs) in the striatum, and on motor cortical electroencephalograms (EEGs) in two monkeys. Striatal LFPs were recorded with a device that allowed us to simultaneously record field potentials and apply drugs by reverse microdialysis at the same site. Administration of the $GABA_A$-receptor antagonist gabazine (SR95531, 10 and 500 μM) induced large-amplitude LFP fluctuations at the infusion site, occurring every 2–5 s for about 2 h after the start of the 20-min drug administration. These events were prevented by cotreatment with a $GABA_A$-receptor agonist (muscimol, 100 μM) or a combination of ionotropic glutamate receptor antagonists (CNQX and MK-801, each given at 100 μM). Gabazine (10 μM) also increased the firing of single neurons recorded close to the injection site, but in most cases there was no correlation between single-neuron activity and the concomitantly recorded LFP signals from the same striatal region. In contrast, intrastriatal application of gabazine increased the correlation between striatal LFPs and EEG, and resulted in the appearance of recurrent EEG events that were temporally related to the striatal LFP events. These data provide evidence that a GABAergic "tone" in the monkey striatum controls the spontaneous activity of striatal neurons, as well as the level of striatal and cortical synchrony.

INTRODUCTION

The striatum is anatomically the most prominent nucleus of the basal ganglia and many of the proposed functions of the basal ganglia have been linked to synaptic processing among cells in the striatum. These functions include possible roles in "focusing" of cortical activity (e.g., Mallet et al. 2005; Ouyang et al. 2007) or in procedural and habit learning (see, e.g., Frank and Claus 2006; Graybiel 2005; Hikosaka et al. 2002; Laubach 2005; Morris et al. 2004; Schultz et al. 2003). The principal striatal neuron types that are involved in these interaction are the medium-sized spiny neurons (MSNs) and the GABAergic and cholinergic interneurons. MSNs receive glutamatergic inputs from the cerebral cortex and from different nuclei of the thalamus (e.g., Djurfeldt et al. 2001; Mallet et al. 2006; Parent and Parent 2006; Slaght et al. 2004; Smith et al. 2004) and send projections to the external and internal pallidal segments, and to the substantia nigra pars reticulata (GPe, GPi, and SNr, respectively), as part of larger basal ganglia–thalamocortical loops (see review by DeLong and Wichmann 2007).

There are several types of GABAergic interneurons. Among them, the parvalbumin-positive "fast-spiking" cells have recently received attention because of their potential role in center–surround-type inhibitory processing (e.g., Mallet et al. 2005). These cells are targeted by glutamatergic inputs from the cerebral cortex (e.g., Mallet et al. 2005) and innervate neighboring MSNs (Kawaguchi et al. 1995; Tepper and Bolam 2004; Tepper et al. 2004). Another important striatal interneuron type is the large cholinergic, "tonically active" aspiny interneuron. These cells receive glutamatergic projections from the intralaminar nuclei of the thalamus (Aosaki et al. 1994; Cragg 2006; Lapper and Bolam 1992; Matsumoto et al. 2001; Meredith and Wouterlood 1990; Sidib é and Smith 1999) and GABAergic inputs from MSN axon collaterals (Anderson et al. 1993; Bennett and Wilson 1998; DeBoer and Westerink 1994; Zackheim and Abercrombie 2005). Cholinergic interneurons mainly target MSNs, with few terminations on GABAergic parvalbumin-containing interneurons (Tepper and Bolam 2004). At the cellular level, acetylcholine may reduce striatal glutamatergic transmission at corticostriatal synapses (Calabresi et al. 1998, 2000; Hernandez-Echeagaray et al. 1998; Malenka and Kocsis 1988; Pakhotin and Bracci 2007; Sugita et al. 1991) and attenuate GABAergic inhibition of MSNs (Koos and Tepper 2002; Perez-Rosello et al. 2005).

All classes of striatal neurons receive prominent inhibitory GABAergic inputs. Although these inhibitory interactions are likely to be essential for striatal processing, details of the actions of γ-aminobutyric acid (GABA) in the striatum and the relevance of a background level of GABA are only beginning to emerge. GABA receptors are found at pre- or postsynaptic locations in almost all neuronal elements in the striatum, but $GABA_A$ receptors are mostly postsynaptic heteroreceptors (Fujiyama et al. 2000; Waldvogel et al. 2004). Presynaptic $GABA_B$ receptors are known to regulate glutamatergic inputs to the striatum (Charara et al. 2000; Kaneda and Kita 2005; Lacey et al. 2005; Nisenbaum et al. 1992).

Studies in rats have shown that MSNs are under tonic GABAergic inhibition (e.g., Kita 1996; Nisenbaum et al. 1992). Based on electrophysiologic studies in vivo in rats, it has been proposed that GABAergic interactions between the fast-spiking interneurons and MSNs may constitute a "center–surround" inhibitory system by which the activity of transtriatal circuits may be focused (Mallet et al. 2005) and that dysfunction of this system may contribute to the development of movement abnormalities in Parkinson's disease (Mallet et al. 2006). Other proposals, such as the notion that GABAergic transmission may regulate the level of synchrony between

Address for reprint requests and other correspondence: O. Darbin, Yerkes National Primate Research Center, Emory University, 954 Gatewood Road, Atlanta, GA 30322 (E-mail: odarbin@emory.edu).

The costs of publication of this article were defrayed in part by the payment of page charges. The article must therefore be hereby marked "*advertisement*" in accordance with 18 U.S.C. Section 1734 solely to indicate this fact.

neuronal elements in the striatum, are currently debated, with both evidence in favor of (Czubayko and Plenz 2002; Koos et al. 2004; Nicola et al. 2004; Taverna et al. 2004; Tecuapetla et al. 2005; Tepper et al. 2004; Tunstall et al. 2002; Venance et al. 2004) and evidence against (Jaeger et al. 1994, 1995; Stern et al. 1998) this possibility.

In the experiments reported here, we investigated the effects of $GABA_A$-receptor blockade in the striatum of awake nonhuman primates, to examine the functional relevance of ambient GABA in the monkey striatum. We found that $GABA_A$-receptor blockade not only increased neuronal spiking in the striatum, as was expected in light of the earlier studies in rodents, but that it also induced the development of striking changes in striatal local field potentials (LFPs) and in the simultaneously recorded motor cortical electroencephalographic (EEG) activity. The results demonstrate that ambient GABA in the monkey striatum strongly inhibits firing activity of striatal neurons and limits synchronous striatal and cortical activity.

METHODS

Animals and surgical procedures

All experiments were carried out in accordance with the National Institutes of Health *Guide for the Care and Use of Laboratory Animals* (ILAC/OLAW 1996) and the PHS Policy on Humane Care and Use of Laboratory Animals (amended 2002). All procedures were approved by the Animal Care and Use Committee at Emory University.

Two female rhesus monkeys (4–6 kg) were studied. The animals were first trained to accept handling by the investigators and to be seated in a primate chair. Both animals were used for the microdialysis and LFP recording sessions. In addition, one of them was used for single-neuron recording studies. After the acclimatization procedures, the animals underwent surgery to prepare them for the subsequent series of recording sessions. Under aseptic conditions and gas anesthesia (1–2.5% isoflurane), stainless steel recording chambers were affixed to the animal's skull, stereotactically aimed at the putamen at a 50° angle from the vertical in the coronal plane. Two silver-ball EEG electrodes were positioned to target the primary motor cortex (M1). The chamber, EEG electrodes, and head-stabilizing bolts were attached to the skull with dental acrylic. The recording sessions began 1 month after surgery.

LFP recording device

LFPs were recorded with ultrafine wires that were incorporated into microdialysis probes (Darbin et al. 2006). The microdialysis probes were acutely introduced into the monkey striatum and were used to deliver drugs via reverse microdialysis. The probes consisted of a 3-mm-long section of microdialysis membrane (Hollow Fiber Bundles; molecular weight cutoff: 13 kDa; Spectra/Por RC; Spectrum Laboratories, Los Angeles, CA), which was closed at one end with epoxy glue (Epoxy; Loctite, Düsseldorf, Germany). The inlet and outlet of the microdialysis probe were composed of two sections of fused silica tubing (length: 15 cm; ID: 40 μm; OD: 103 μm; Polymicro Technologies, Phoenix, AZ), placed inside the membrane. Two insulated wires (Nichrome/Formvar wire, A-M Systems, Carlsborg, WA; bare diameter: 0.0020 in.; coated diameter: 0.0026 in.) were also inserted into the membrane. The wires were inserted into the membrane alongside the inlet- and outlet tubes and positioned so that the wire tips were separated by 2.5 mm. The impedance of individual wires, measured at 1,000 Hz, was about 250 kΩ, and the entire bipolar system had an impedance of about 500 kΩ. Measured at 30 Hz, the impedance was about 750 kΩ for single wires and about 1.5 MΩ for the bipolar electrode system.

The probe assembly was placed into a polyimide sleeve (OD: 0.25 mm; length: 12.5 cm; MicroLumen, Tampa, FL). The recording wires were then connected via an impedance adaptor (Model HZP High Impedance Probe, Grass, West Warwick, RI) to an amplifier (Model 8–16 Amplifier; Grass) for bipolar (differential) amplification and filtering (0.1–75 Hz). In all cases, the more proximal wire was connected to the positive (noninverting) pole of the amplifier. We recently published a detailed description of the assembly and characteristics of this system (Darbin et al. 2006).

Microdialysis/LFP recording experiments

For each recording session, the animal was seated in a primate chair, with its head fixed in position. In preliminary sessions, we delineated the borders of the striatum by electrophysiologic mapping with conventional tungsten microelectrodes (impedance: 0.7–1 MΩ, measured at 1,000 Hz; FHC, Bowdoinham, ME) and standard electrophysiologic single-unit recording methods (see also Soares et al. 2004). For each of the microdialysis/LFP recording experiments, we targeted the posterior portion of the putamen between A10 mm and A14 mm, based on the previously generated electrophysiological maps. Each experiment was performed in a previously unused location in the striatum. Prior to the microdialysis experiment, the microdialysis/LFP recording system was perfused overnight with distilled water at a rate of 0.5 μl/min delivered by gastight 1-ml syringes (CMA, Solna, Sweden), operated by a microinfusion pump (CMA/120; CMA). Thirty minutes before insertion into the brain, the system was perfused with artificial cerebrospinal fluid (aCSF; composition in mM: 147.0 Na^+, 4.0 K^+, 1.0 Mg^{2+}, 1.2 Ca^{2+}, and 153.2 Cl^-; CMA), at a rate of 1 μl/min. Transitions between perfusion solutions were accomplished using a liquid switch (CMA/110; CMA). The probe was mounted to a microdrive (MO-95B, Narishige, Tokyo, Japan) and slowly lowered through a guide tube (modified CMA/11 guide system; CMA) through the dura, into the brain. After a 60-min equilibration period, we started the LFP recordings. For this, the recording wires within the microdialysis system were connected via an impedance adaptor to an amplifier for amplification and filtering (see earlier text). The same amplifier and filter conditions were also used for the bipolar EEG recordings that were made simultaneously with the LFP recordings, using the implanted epidural EEG electrodes. The amplified LFP and EEG signals were digitized (sampling rate: 500 Hz/channel) and stored to computer disk via a data acquisition system (Power 1401 with Spike2 interface; CED, Cambridge, UK) for later off-line analysis. Throughout the experiments, the behavior of the animal was carefully observed and videotaped. Together with EEG monitoring, the behavioral observations demonstrated that the animals were fully awake during the experiments.

Preparation of drug solutions and protocol of administration

All agents used in this study were freshly dissolved in aCSF. In the first set of microdialysis/LFP recording experiments, we examined the effects of local intrastriatal application of the $GABA_A$-receptor antagonist gabazine [2-(3-carboxypropyl)-3-amino-6-methoxyphenylpyridazinium bromide (SR95531), Tocris Bioscience, Ellisville, MO; 0.1–500 μM] or of the $GABA_B$-receptor antagonist CGP55845 [(2*S*)-3-[[(1*S*)-1-(3,4-dichlorophenyl)ethyl]amino-2-hydroxypropyl](phenylmethyl)phosphinic acid; Tocris Bioscience; 100 μM]. These drugs were administered for 20 min, starting 40 min after the beginning of the recording session. In other experiments, gabazine was applied together

with the $GABA_A$-receptor agonist, muscimol (Sigma, St. Louis, MO; 100 μM), or with a combination of the ionotropic glutamate receptor blockers, MK-801 [(+)-5-methyl-10,11-dihydro-5H-dibenzo[a,d]cyclohepten-5,10-imine maleate] and CNQX (6-cyano-7-nitroquinoxaline-2,3-dione) (100 μM each, blocking *N*-methyl-D-aspartate and α-amino-3-hydroxy-5-methyl-4-isoxazolepropionic acid/kainate receptors, respectively; Tocris Bioscience). Perfusion with these drugs began 20 min before, and continued throughout, the administration of gabazine (10 μM). The volume of tissue that is affected by the drugs was not directly investigated in this study. A previous study of this topic reported that such effects can be noted at distances $\leq$1 mm away from the microdialysis probe (Westerink and De Vries 2001). It is difficult to generalize such estimates because they are strongly dependent on the specific pharmacologic properties of the drugs under study, but it is very likely that the direct pharmacologic effects of the drugs used in our study occurred within the striatal tissue surrounding the probes.

Combined recording of single-cell activity, LFP signals, and EEG signals

We found that gabazine infusion resulted in prominent LFP changes (see following text). This prompted us to study the effects of gabazine on the activity of single striatal neurons, to explore how this is related to the LFPs. For these studies, a multielectrode microdrive (NAN Instruments, Nazareth, Israel) was used to introduce both the microdialysis/LFP recording device and a standard tungsten microelectrode (see earlier text) into the striatum. This device provides independent control of the depths of the two probes. The microelectrode and microdialysis/LFP recording device were lowered into the brain through separate guide tubes. The electrodes were introduced 1–3 mm lateral or medial to the microdialysis system. LFP signals were amplified as described earlier. The electrical signals recorded through the microelectrodes were amplified (DAM-80; World Precision Instruments, Sarasota, FL), filtered (400–10,000 Hz; Krohn-Hite, Brockton, MA), displayed on a digital oscilloscope (DL1540; Yokogawa, Tokyo, Japan), and made audible via an audio amplifier. The amplified signals from the microelectrodes were digitized at 25,000 Hz (Power1401 and Spike2, CED) and stored to computer disk, along with the LFP and EEG signals described earlier. The electrical activity from the microelectrode was sampled before and 20–60 min after the start of the gabazine (10 μM) administration through the microdialysis/LFP recording device, along with LFP and EEG signals. In these experiments, gabazine was applied repeatedly (two to three times per experiment, at 30-min intervals) to maintain the stability of the observed LFP changes.

A frequent bias in in vivo striatal recordings results from the fact that MSNs have very low firing activity, whereas several types of interneurons fire spontaneously. This may lead to a disproportionate representation of interneurons. To minimize this bias, the electrodes were advanced along the electrode path through the striatum in 250-μm steps, with pauses at each location for several minutes, even if no neuronal activity was detected initially. This allowed us to detect neurons of low activity, along with neurons with a tonic firing pattern. Before and after gabazine application, we recorded from all of the neurons encountered in the striatum with the recording electrode. This procedure did not completely eliminate recording biases, but it reduced the likelihood that there were substantial differences in the distributions of neuron types sampled before and after gabazine administration.

Analysis

ANALYSIS OF STRIATAL LFPS. Gabazine induced recurring large-amplitude fluctuations in the striatal LFP record. We analyzed the LFP data with custom-designed algorithms in Matlab (The MathWorks, Natick, MA). The stored LFP signals were down-sampled to 241 Hz, digitally filtered between 0.5 and 35 Hz (four-pole Butterworth filter), and then segmented into 10-s "frames." Each frame was screened visually and frames with movement artifacts were rejected. Such artifacts were infrequent, and irregular in shape, and were therefore easily distinguished from the recurring stereotyped LFP events. LFP events were identified on the basis of a threshold criterion. The events were displayed on a computer screen and the beginning and the end of each individual gabazine-induced event was marked by visual inspection. The computer program reported the overall duration of the series of gabazine-induced changes in each experiment, the number of LFP events, and the average duration of the events in consecutive 5-min epochs, starting with the moment of injection of gabazine.

In addition to the individual LFP events, we also observed closely spaced strings of large-amplitude LFP fluctuations that lasted for >5 s. Facial movements and other behavioral changes were noted during a few of these experiments and confirmed later in the videotaped records.

ANALYSIS OF NEURONAL FIRING RATES AND CORRELATION BETWEEN SPIKING ACTIVITY AND LFPS. Neuronal spikes were identified in the stored neuronal signal traces by applying a waveform-matching spike-sorting algorithm with subsequent principal component analysis (Spike2). The timing of spike occurrences was imported into Matlab and expressed in terms of interspike intervals (ISIs). The relationship between LFPs and changes in the neuronal spiking rates of simultaneously recorded neurons was explored with cross-correlation analyses of the LFP data and the ISI series, convolved with a Gaussian kernel (sigma = 50 ms). The 1st and 99th percentiles of data from cross-correlograms obtained from 100 shuffled representations of the ISI data streams were used as the limits of the confidence interval. Although it would have been highly interesting to examine separate groups of neurons in the striatum, we did not attempt to separate the recorded neurons into MSNs or interneurons because it is not clear whether the criteria that can be used for the classification of striatal neurons in the normal state (such as the firing frequency, the duration of the action potential, or the degree of regularity of firing) still apply after blockade of $GABA_A$ receptors. Instead, the analysis of the effects of gabazine on striatal neuronal activity is based on analyses of the activities of the entire population of cells recorded before and after drug administration.

EEG ANALYSIS AND CORRELATIONS TO STRIATAL LFPS. Prior to further processing, EEG records were screened by visual examination of 10-s frames (see earlier text) and frames with artifacts were rejected; thus <1% of the total length of the record was rejected. The remaining sections of EEG were analyzed to determine whether the LFP events in the striatum were associated with EEG changes.

We first calculated the cross-correlation between the EEG signals and the striatal LFP signals to determine the temporal progression of the LFP–EEG interactions. For this, the absolute values of cross-correlograms (calculated with a lag of $\pm$1,000 ms), based on successive 10-s segments of data, were integrated and averaged over 5-min periods. The data describing the correlations during and after drug administration were expressed as a percentage of the basal values observed before drug administration.

To analyze the direct relationship between the LFP events and events seen in the cortical EEG, we also calculated averages of 2-s EEG segments, centered on individual LFP events. For the display in Fig. 10, these segments were averaged over consecutive 20-min periods to characterize the time course of the effect of gabazine administration.

STATISTICS. Throughout this study, we used nonparametric methods for statistical testing. The data were expressed as medians with 25th–75th percentiles. Kruskal–Wallis and Mann–Whitney tests were

used for between-group comparisons. Correlation coefficients were calculated using the Spearman correlation test (Siegel 1989). A P value of <0.05 was considered to be evidence of a significant difference.

RESULTS

Gabazine induces LFP changes

The microdialysis-LFP recording device allowed us to administer drugs by reverse microdialysis and to record simultaneous local field potentials at the same location. Local administration of gabazine at concentrations of 10 μM ($n = 8$ experiments; Figs. 1, 2, and 4) and 500 μM ($n = 6$; Figs. 2, 3, and 4) with this device induced large repetitive LFP events in the striatum. These events occurred as discrete entities that were of much higher amplitude than that of the background activity. No such events were found at low gabazine concentrations (0.1 μM; $n = 6$), in control recordings in which aCSF was infused ($n = 6$), or following the administration of the $GABA_B$-receptor antagonist CGP55845 (100 μM; $n = 4$; Fig. 6). Note that the occasional spikelike fluctuations in the LFP signal, prior to drug infusion (e.g., see Fig. 1, arrow), are movement artifacts. Such artifacts were easily distinguished from the LFP events and artifact-containing segments were excluded from the quantitative analyses.

Characteristics of gabazine-induced changes in LFP recordings

The gabazine concentration influenced the shape, duration, amplitude, and frequency (Kruskal–Wallis test, $\chi^2 = 21.57$, df = 3, $P < 0.001$; Fig. 5) of the LFP events. As shown in Figs. 2 and 5, gabazine at 10 μM induced events with a median duration of 0.47 s (range 0.33–0.64 s), whereas gabazine at 500 μM induced longer events (median event duration of 0.74 s, range 0.66–0.83 s) that were more complex and superimposed on recurrent shifts in baseline potential. The increase in event duration as drug concentration increased was statistically significant (Mann–Whitney U test: $U_{10\mu M} = 26{,}017$, $U_{500\mu M} = 33{,}667$, $z = -10.39$, $P < 0.001$; Fig. 5*C*). In most of the experiments with gabazine 500 μM (five of six experiments, 83%), we also observed the intermittent occurrence of episodes of more sustained activity, starting immediately after a large-amplitude LFP fluctuation and continuing for several seconds (median, 24 s; range 15–57 s; Fig. 3).

In any given experiment, the durations and shapes of individual LFP events changed over time and these changes were

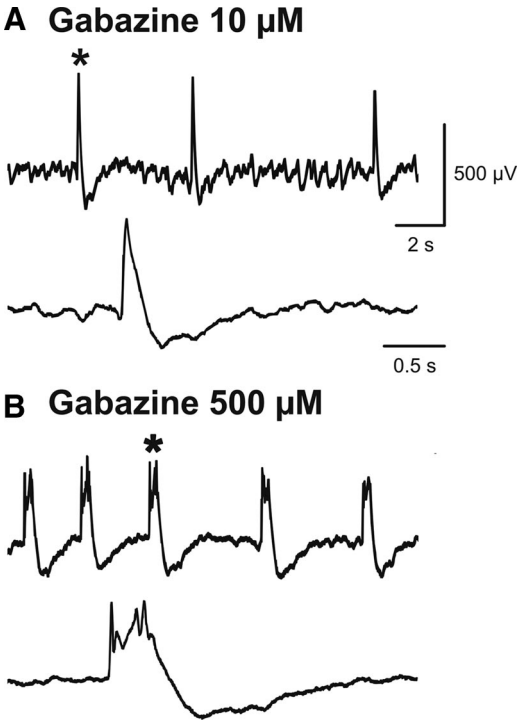

FIG. 2. Representative samples of striatal LFP events of different shapes recorded after local gabazine application at 10 μM (*A*) and at 500 μM (*B*). *Bottom traces*: the events labeled with an asterisk at a higher time resolution. The voltage and time calibration bars shown in *A* also apply to *B*.

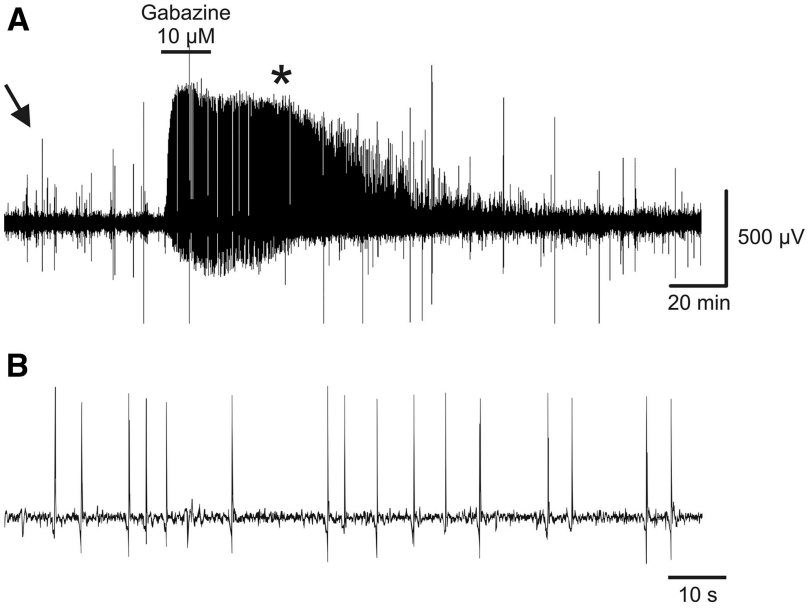

FIG. 1. Effects of local application of gabazine on striatal local field potentials (LFPs). *A*: example record of bipolar LFP recordings before, during, and after perfusion of gabazine (10 μM). The arrow marks a movement artifact. The trace in *B* shows a shorter data segment at higher time resolution taken from the same record (marked by asterisk in *A*). The voltage calibration shown in *A* also applies to *B*.

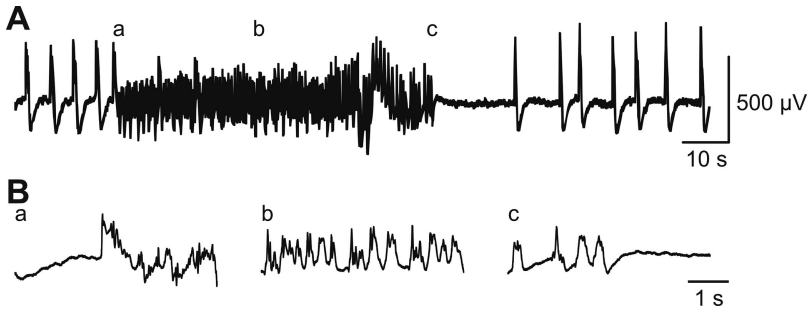

FIG. 3. *A*: example of a sustained LFP event recorded in the striatum after local application of gabazine (500 μM). The sections marked *a*, *b*, and *c* in the trace in *A* are shown at higher time resolution in *B*.

also dependent on the concentration of gabazine. As shown in Fig. 5*C*, with gabazine at 10 μM, the durations increased over the first 30 min to reach a maximum of 700 ms (Spearman correlation, $r = 0.624$, $P < 0.001$), followed by gradual shortening over the next 110 min of recording (Spearman correlation, $r = -0.638$, $P < 0.001$). With 500 μM gabazine, the duration increased faster and reached a plateau value of 700–800 ms that was maintained for the rest of the recording session (Spearman correlation, time 5–140 min, $P > 0.1$). The concentration of gabazine was also related to the size of the induced LFP events in individual experiments. Using cumulative dosing of gabazine, we showed that the amplitude of the LFP events increased as gabazine concentrations in the infusate increased ($n = 3$, Fig. 4).

Increasing the drug concentration also increased the total number of events per experimental session (Kruskal–Wallis test: $\chi^2 = 21.57$, df = 3, $P < 0.001$; Fig. 5*A*) and their frequency at any given point in the recording period (Mann–Whitney *U* test: $U_{10\mu M} = 27{,}545$, $U_{500\mu M} = 38{,}884$, z = −13.66, $P < 0.001$; Fig. 5*B*). The analysis in Fig. 5 shows that the number of events seen during the recording period after gabazine 500 μM (Fig. 5*A*, median 2,356; range 2,263–3,300 events) was more than twice that seen with 10 μM (median 1,060, range 762–1,443 events; Mann–Whitney *U* test: $U_{10\mu M} = 37$, $U_{500\mu M} = 54$, z = 2.781, $P < 0.005$). At 10 μM, gabazine-induced events reached their peak frequency (about 60 events/5 min) 10 min after the beginning of the drug administration, followed by a gradual decline over the next 105 min (Spearman correlation $r = -0.614$, $P < 0.001$; Fig. 5*B*). In contrast, with gabazine at 500 μM, the frequency of these events continued to increase (to an average of 110 events/5 min) through the first hour after the start of the drug infusion (Spearman correlation, $r = -0.587$, $P < 0.002$) and did not significantly decline over the remainder of the recording session (Spearman correlation, $P > 0.1$; Fig. 5*B*).

Effects of coadministration of gabazine with other drugs

As shown in Fig. 6, coadministration of gabazine (10 μM) with the $GABA_A$-receptor agonist muscimol (100 μM, $n = 6$) or with a combination of ionotropic glutamate receptor antagonists (MK-801 and CNQX, each at 100 μM, $n = 4$), given for 40 min, starting 20 min before the gabazine application, completely prevented the gabazine-induced LFP events, but did not affect the amplitude of the background LFP signals. The gabazine-induced effects persisted in the presence of the $GABA_B$-receptor antagonist CGP55845 (100 μM).

Gabazine-induced effects on neuronal firing

Using a microdrive capable of independently driving multiple probes, we recorded from cells in the vicinity of the microdialysis/LFP recording device before and after administration of gabazine (10 μM). Under control conditions, all of the recorded neurons fired at rates <1 spike/s ($n = 50$ cells) and are therefore likely to have been MSNs. After administration of gabazine ($n = 26$ cells), the average rate increased to 1.9 spikes/s (Mann–Whitney *U* test: $U_{control} = 30$, $U_{10\mu M} = 64$, z = 5.83; $P < 0.005$), with 9 cells firing faster than 3/s, and 3 cells firing at rates >10 spikes/s. Although the average discharge rate increased after gabazine administration, there was no clear temporal correlation between the LFP events and neuronal firing patterns in 24/26 cells, as is shown in the example recording in Fig. 7. These cells were recorded during a 90-min period following a single 20-min infusion of gabazine (10 μM). In the other two cells, gabazine exposure led to brief episodes of correlation between the LFP signal and neuronal firing (Fig. 8). Both of these cells fired at high rates (median rates of 28.5 and 40.1 spikes/s, respectively) and were recorded after repeated 20-min applications of gabazine to maintain the same amplitude of the LFPs (two and three times, respectively,

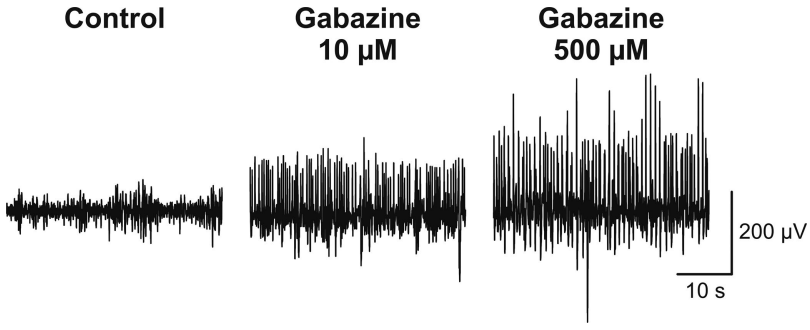

FIG. 4. Effects of gabazine concentration on the amplitude of evoked LFP events. The figure shows striatal LFP recordings demonstrating changes in the amplitude of LFP events during an example experiment in which progressively higher doses of gabazine were applied.

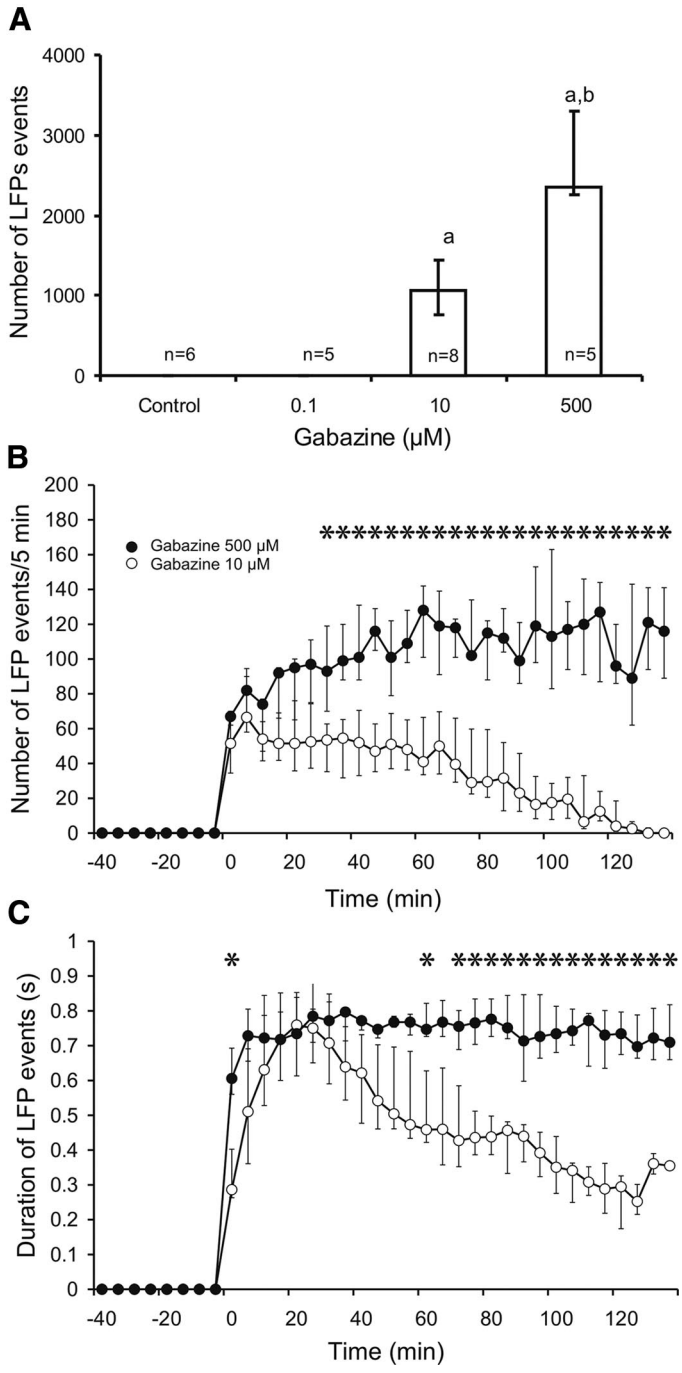

FIG. 5. Characterization of gabazine-induced striatal LFP events. *A*: effect of striatal gabazine administration on the total number of LFP events. *a*: $P < 0.05$, gabazine exposure vs. control, Mann–Whitney *U* test; *b*: $P < 0.05$ and 10 μM, gabazine exposure at 500 μM ($n = 6$) vs. gabazine exposure at 10 μM ($n = 8$). *B*: time course of the number of LFP events (measured in 5-min intervals) after infusion of gabazine. *C*: changes in the duration of individual LFP events, evoked by infusion of gabazine. *$P < 0.05$, drug effect vs. control, Mann–Whitney *U* test. The long-lasting sustained LFP events (see example in Fig. 4) were not included in this analysis. In *B* and *C*, experiments with gabazine 10 μM are depicted as open circles (○), whereas experiments with gabazine 500 μM are shown as filled circles (●). Data points in *A*, *B*, and *C* represent medians; error bars represent the 25th–75th percentile range.

over 2 h). Under these conditions, LFP events occurred at a faster rate than in the experiments with only a single 20-min exposure to gabazine (see Fig. 7 for comparison).

Gabazine-induced changes in the correlation between motor cortex EEG and striatal LFPs

In all experiments, we recorded EEG signals from motor cortex (abbreviated as M1-EEG in Figs. 9 and 10) along with the LFP signals. Visual examination of the EEG after administration of gabazine 500 μM ($n = 6$) in the striatum revealed the appearance of discrete events that were correlated in time with the occurrence of the striatal LFP events (Fig. 9). Such events were not apparent in the raw traces after the 10 μM gabazine ($n = 8$), but statistical evaluation with cross-correlation methods showed that gabazine administration at both concentrations increased the overall correlation between the EEG and LFP signals. Using integrated absolute cross-correlograms as a measure of correlation, we found that the increase was significant at both 10 and 500 μM gabazine (Kruskal–Wallis test, 10 μM: $\chi^2 = 177$, df = 35, $P < 0.001$; 500 μM: $\chi^2 = 93$, df = 35, $P < 0.001$; Fig. 9*B*), and that its magnitude

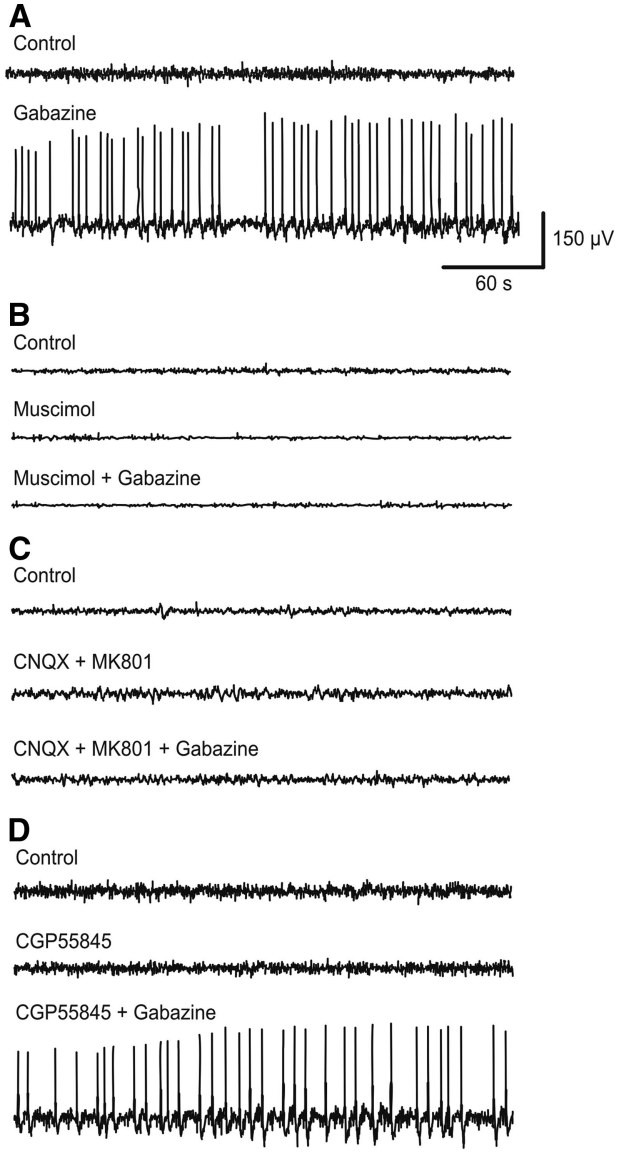

FIG. 6. Example recordings from experiments in which either gabazine (10 μM) was infused alone (*A*) or in combination with other drugs (*B–D*). The time and amplitude calibration bars shown in *A* apply to all parts of the figure.

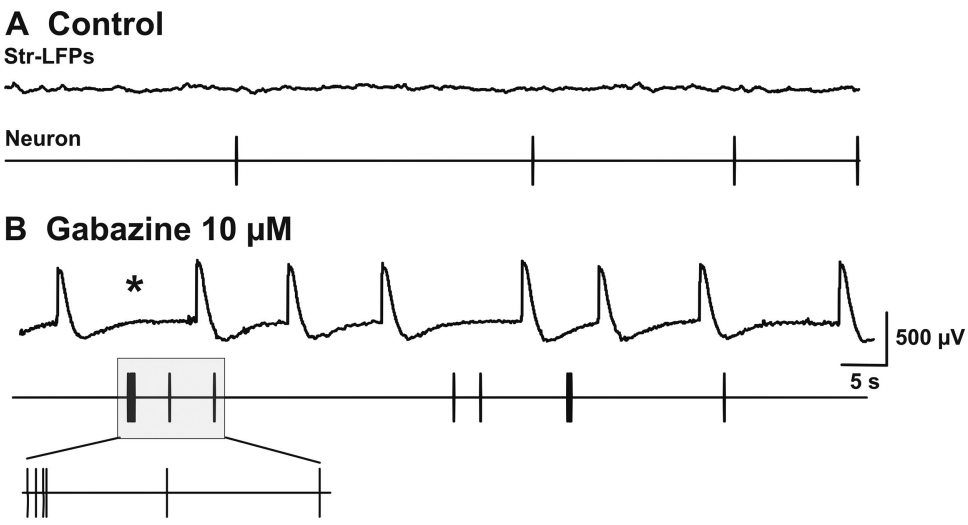

FIG. 7. Examples showing the relationship between the timing of neuronal spiking (trace labeled "Neuron") and simultaneously recorded striatal LFPs (trace labeled "Str-LFP") under control conditions (*A*) and after administration of gabazine 10 μM (*B*). *B*, *bottom trace*: an expanded view of temporal spiking activities after gabazine administration.

depended on the drug concentration (Mann–Whitney U test: $U_{10\mu M} = 161$, $U_{500\mu M} = 280$, z = 9.954, $P < 0.005$; Fig. 9*B*).

We further analyzed the relationship between the LFP events and EEG signals, by averaging segments of EEG occurring around the peaks of the LFP events (Fig. 10; see METHODS). This analysis showed that the occurrence of EEG events was temporally linked to the striatal LFP events. As shown in the example in Fig. 10 (*top trace*), averaging over 20-min time periods demonstrated EEG changes with both gabazine concentrations. As expected, 500 μM gabazine induced stronger cortical involvement than 10 μM gabazine (Fig. 10, *bottom trace*).

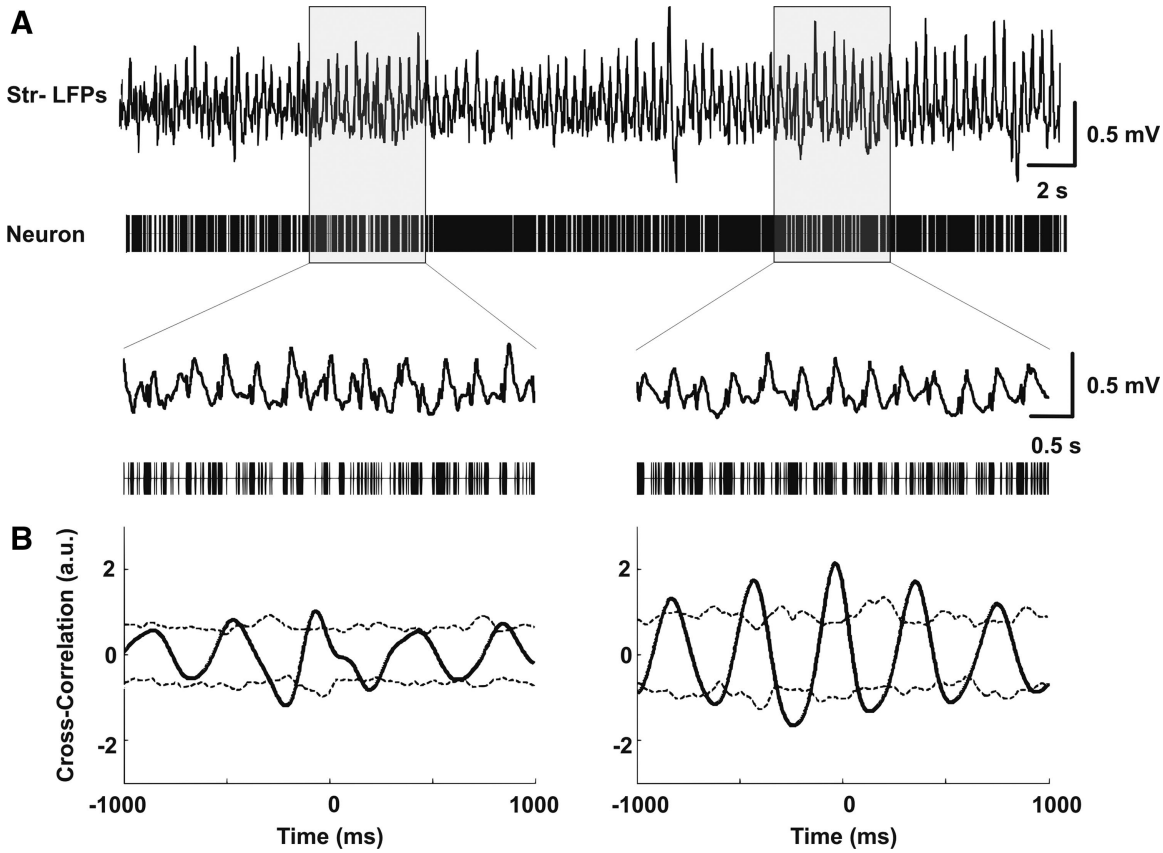

FIG. 8. Striatal activity of a single-unit activity of a striatal neuron firing at a relatively high discharge rate after administration of gabazine 10 μM. *A*: a 40-s segment of a striatal LFP trace (labeled "Str-LFPs"; *top trace*) recorded together with the firing activity of a cell (labeled "Neuron") in the vicinity of the microdialysis probe. *B*: correlation between the LFP signal and neuronal activity. The solid lines represent the cross-correlograms between the LFP signal and the neuronal activity. The dashed lines represent the 1st and 99th percentiles of a population of 100 cross-correlograms generated by correlating the LFP data with shuffled representations of the neuronal data (see METHODS for details). This cell was one of 2 cells (from a total of 26 cells) whose activity went in (*right*) and out (*left*) of correlation with the LFP signal.

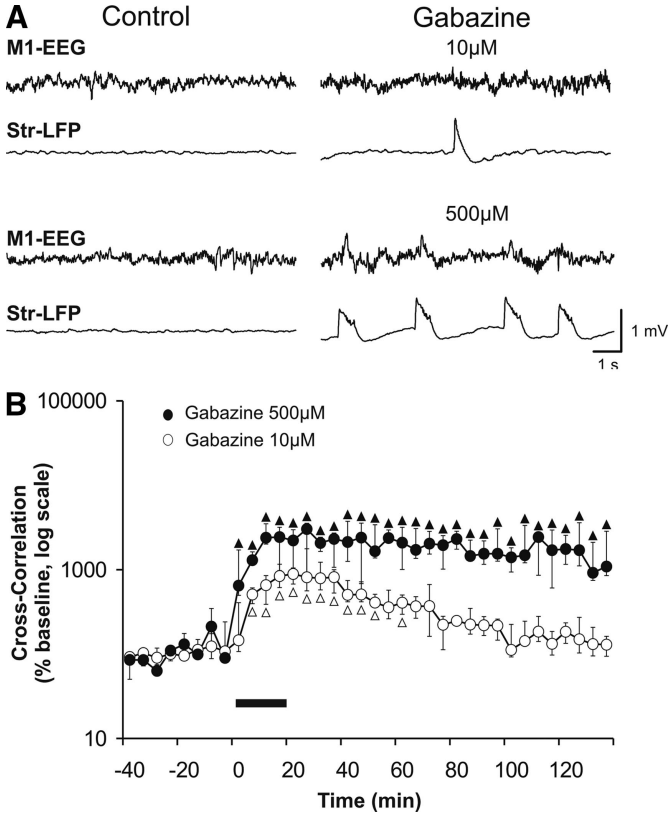

FIG. 9. Striatal infusion of gabazine induces electroencephalographic (EEG) changes. Samples of simultaneously recorded motor cortical EEG ("M1-EEG") and striatal LFPs (labeled "Str-LFP") are shown in *A* before (*left*) and after (*right*) administration of gabazine 10 μM (*top traces*) or 500 μM (*bottom traces*). *B*: plot showing the progression of the integrated absolute cross-correlation between the 2 signals over time (see METHODS). Data points represent medians and error bars represent the 25th–75th percentile ranges. Experiments with gabazine 10 μM are depicted as open circles (○), whereas experiments with gabazine 500 μM are shown as filled circles (●). Open and closed triangles mark data points with significant peaks in the cross-correlograms ($P < 0.05$, Mann–Whitney *U* test).

Behavioral changes induced by the striatal gabazine infusions

Video images of the animals recorded throughout the gabazine infusions were carefully examined. In most sessions, gabazine administration had no behavioral consequences. However, in two of six sessions in which the highest concentration of gabazine (500 μM) was used, we observed facial movements, including eye blinking, chewing, teeth grinding, and excessive salivation. These behaviors started approximately 60 min after beginning the drug infusion and continued for several hours.

DISCUSSION

These data show that intrastriatal administration of the specific $GABA_A$-receptor antagonist gabazine increases the spiking activity of striatal neurons and evokes recurrent large-amplitude LFP fluctuations, parallel to similar changes in motor cortical EEG. Striatal LFP events were not induced by administration of the $GABA_B$-receptor antagonist CGP55845. Pretreatment with the $GABA_A$-receptor agonist muscimol, or with a combination of the ionotropic glutamate receptor antagonists MK-801 and CNQX, prevented the development of the gabazine-induced striatal LFP events. These studies show that baseline $GABA_A$-receptor activation by endogenous GABA under physiologic conditions reduces the activity of striatal neurons and that ambient GABA in the striatum may act to restrain the level of synchrony of activity in the basal ganglia–thalamocortical circuitry.

Effects of ambient GABA on single-cell activity

Most GABAergic interactions in the striatum involve terminals of intrinsic striatal neurons, including MSNs, which represent the majority of all striatal neurons (see, e.g., Rymar et al. 2004), and several classes of GABAergic interneurons (Cowan et al. 1990; Kawaguchi 1993; Mallet et al. 2005; Tepper et al. 2004; Wu and Parent 2000). Commensurate with the large number of striatal GABAergic synapses, $GABA_A$ receptors are ubiquitous in the striatum (Riedel et al. 1998; Waldvogel et al. 2004), with the majority found at postsynaptic sites (Fujiyama et al. 2000).

In line with previous in vitro studies in the rat striatum (Kita 1996; Nisenbaum et al. 1992), we found that intrastriatal administration of a $GABA_A$-receptor antagonist increased the average firing rates of striatal neurons, demonstrating that $GABA_A$ receptors tonically inhibit striatal cells in the monkey. Althoughe we are unable to establish unequivocally the identity of the recorded neurons in the in vivo recordings, several points can be raised to address this question. Given the very

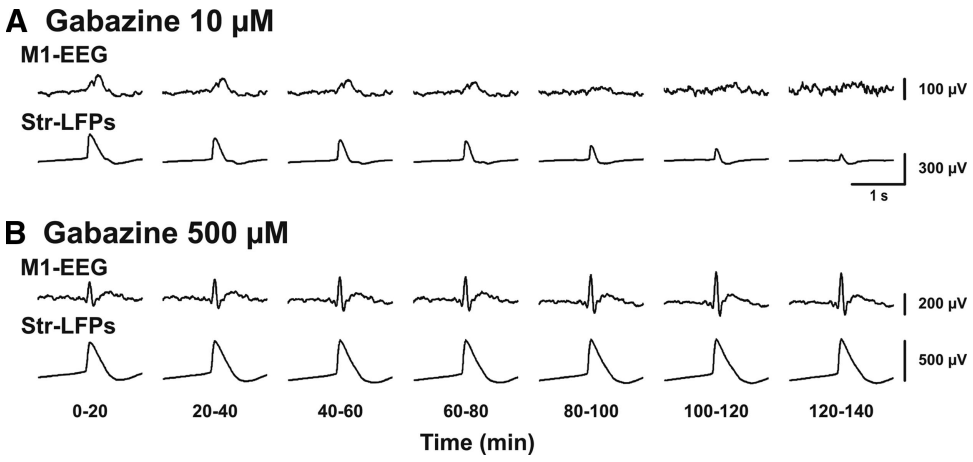

FIG. 10. Analysis of simultaneously recorded motor cortical EEG ("M1-EEG") and striatal LFP signals ("Str-LFP") after gabazine administration at 10 μM (*A*) or 500 μM (*B*). Each of the displayed segments represents respective averages of all available 2-s segments of data, centered on the peak of the striatal LFP events, and recorded during the 20-min intervals indicated at the *bottom* of the figure. Note the different ordinate calibrations for the 2 parts of the figure.

low firing rates, and the statistical likelihood of encountering MSNs, most of the neurons recorded in the pregabazine phase of the recording sessions can be assumed to be MSNs. It is likely that the majority of neurons in the postgabazine sample of neurons were also MSNs because the median postgabazine firing rate was 1.9 spikes/s, which is below the average spontaneous firing rate of tonically active neurons or fast-spiking cells (see, e.g., Aosaki et al. 1994, 1995; Morris et al. 2004; Raz et al. 1996). However, cells spiking at higher rates were also found, suggesting that at least some of the postgabazine recordings may have been from tonically active cholinergic cells or other interneurons.

Gabazine is likely to have acted at $GABA_A$ receptors on striatal neurons that were at baseline exposed to endogenous GABA. The gabazine effects may have differed between the types of neurons and synaptic sites at which it acted. MSNs receive GABAergic axon collaterals from neighboring MSNs (Kawaguchi 1993; Loopuijt and van der Kooy 1985), but the low intrinsic activity of MSNs and the fact that the collaterals terminate distally on dendrites of other MSNs suggest that axon collateral interactions between MSNs are relatively weak (Czubayko and Plenz 2002; Jaeger et al. 1994, 1995; Koos et al. 2004; Stern et al. 1998; Taverna et al. 2004; Tecuapetla et al. 2005; Tepper et al. 2004; Tunstall et al. 2002; Venance et al. 2004), so that $GABA_A$-receptor blockade at these sites is less likely to have had prominent effects. It is more likely that most GABAergic inhibition of MSNs originates from GABAergic interneurons and that gabazine exerted prominent effects at these sites. The activity of (fast-spiking) interneurons is substantially higher than that of MSNs and they provide synaptic input closer to the soma of MSN cells (Gustafson et al. 2006; Hellgren Kotaleski et al. 2006; Koos et al. 2004; Mallet et al. 2005; Tepper et al. 2004). GABAergic input from fast-spiking interneurons to MSNs may be influenced by glutamatergic inputs from cortex and thalamus and may provide feedforward inhibition to MSNs (Mallet et al. 2005; Parthasarathy and Graybiel 1997).

GABAergic inputs to striatal interneurons also originate from several sources and GABA-receptor blockade at these sites, counteracting an ambient GABAergic tone, may have contributed to the changes in neuronal spiking. Given the preceding considerations, the inputs from GABAergic interneurons are likely to be substantially more important than those from MSNs. Cholinergic interneurons receive GABAergic input predominately from MSN collaterals (Martone et al. 1992). Interestingly, despite the aforementioned low intrinsic activity along MSN collaterals, the GABAergic tone afforded by these inputs onto cholinergic cells appears to be substantial (Zackheim and Abercrombie 2005).

The influence of other striatal systems exposed to ambient GABA to the effects seen in our results is more difficult to gauge. It is known that neurons in the external pallidal segment (GPe) send a GABAergic projection to the striatum (Bevan et al. 1998; Kita 2007; Sadek et al. 2007; Sato et al. 2000; Smith and Parent 1986), but the cellular target of this projection is not clear. Nonneuronal sources of GABA release (Campbell et al. 1993) may also contribute to the overall GABA level, and thus to the effects of gabazine on cellular firing.

Effects of ambient GABA on striatal LFP and cortical EEG signals

Local intrastriatal application of gabazine had prominent effects on striatal LFPs. We have previously shown that striatal LFPs recorded under the conditions used in this study are not correlated with cortical EEGs (see also Darbin et al. 2006). The bipolar montage used in our LFP recordings minimizes the influence of distant electrical activity, which would reach each electrode similarly by volume conduction. Considering the ratio between the amplitude of the gabazine-evoked LFP events and the amplitude of the background activity recorded in the striatum before gabazine exposure, it is likely that the gabazine-related events were the product of synchronous activities generated close to the LFP recording electrode (see also Bedard et al. 2004; Brown and Williams 2005; Goldberg et al. 2004). We will consider several possibilities to explain the LFP and EEG findings.

The general lack of correlation between the LFP events and simultaneously recorded single-unit activity suggests that synchronous subthreshold synaptic currents generated in the vicinity of the electrode were a major contributor to the LFP signals (see also discussions in Darbin et al. 2006; Galvan et al. 2002; Kaur et al. 2004; Norena and Eggermont 2002). $GABA_A$-receptor blockade with gabazine is likely to have interrupted most synaptic interactions among neurons intrinsic to the striatum. Thus it is likely that the postgabazine LFP events were in large part driven by synchronous activities of striatal afferents, resulting in similarly synchronous postsynaptic potentials. This is further supported by the fact that ionotropic glutamate receptor antagonists blocked the emergence of the gabazine-induced LFP events (Bracci et al. 2004; Hu and Wang 1988; Sandstrom and Rebec 2003), likely acting at synapses of glutamatergic inputs originating from cortex (Kemp and Powell 1970) or thalamus (Smith et al. 2004).

We also found that blockade of striatal $GABA_A$ receptors increased the correlation between the striatal LFP and motor cortical EEG signals. This is most easily explained in terms of the influence of striatal (and thus basal ganglia) output on cortical activity. However, the fact that the correlated EEG/LFP activities occurred without clear entrainment of striatal output neurons by the LFP events suggests that striatal gabazine administration did not directly produce oscillatory spiking activity in individual striatal output neurons, but that it may have primarily acted to increase striatal output, which then led to the emergence of rhythmic synchronous activity in areas outside of the striatum, for instance, cortex or thalamus. The LFP events would have resulted from synaptic activity at the sites of the returning glutamatergic inputs from cortex or thalamus.

Another possibility to consider is that at least some of the LFP activity was generated by spontaneous burst firing of striatal interneurons. In fact, the two cells that exhibited a firing pattern that was temporarily correlated with the LFP signals showed high firing rates and may have been striatal interneurons. It is known that some striatal interneuron types, specifically cholinergic and fast-spiking interneurons, are capable of generating rhythmic bursts at rates that are comparable to those at which the LFP events occurred in our study (Bennett and Wilson 1999; Bracci et al. 2003; Kawaguchi 1993; Kita 1993; Koos and Tepper 1999, 2002; Pisani et al. 2007; Plenz and

Kitai 1998). Importantly, these interneurons may express synchronized firing patterns (e.g., Bauer et al. 1995; Collins et al. 2001; Courtemanche et al. 2002; Donoghue et al. 1998; Takahashi and Straschill 1981), which may have played a role in the generation of the LFP events, although this would make the observed EEG changes difficult to explain.

The presence of large LFP events that were not strongly related to neuronal spiking could also be explained by changes in the activity of larger ensembles of striatal cells not detectable in the recording from individual cells, but was sufficient to alter LFP recordings. Such changes in ensemble activity could be transmitted to sites outside of the striatum and could act to entrain thalamic or cortical regions into the oscillatory activity that was generated in the striatum. This possibility could be tested in future experiments through multi-electrode recordings in the striatum and other elements of the basal ganglia–thalamocortical circuitry.

Effects of $GABA_A$-receptor blockade on behavior

In most of our experiments, gabazine administration in the striatum did not trigger behavioral changes. However, in two experiments in which the highest concentration of gabazine was used, facial twitching and other behavioral effects were seen, suggesting that GABAergic inhibition in the striatum may be one of the mechanisms that normally prevent excessive movements (Crossman et al. 1988; Marsden et al. 1975; Nakamura et al. 1990; Yoshida et al. 1991). It is possible that reduced inhibition in the striatum may contribute to movement disorders such as some forms of dystonia (Fredow and Loscher 1991; Kreil and Richter 2005; Loscher and Horstermann 1992; Nobrega et al. 1995; Pratt et al. 1995; Richter and Loscher 1993; Yoshida et al. 1991) or myoclonus (Darbin et al. 2000). GABAergic inhibition in the striatum may also act to inhibit seizure generation (Dematteis et al. 2003) or propagation (e.g., Benedek et al. 2004; Biraben et al. 2004; Bouilleret et al. 2005; Sasaki et al. 2000; Vercueil et al. 1999). Our experiments show that local blockade of striatal $GABA_A$ receptors has substantial effects on the function of the entire basal ganglia–thalamocortical system. Modulation of striatal GABA levels may therefore represent a pharmacological target of interest in the treatment of movement disorders or seizures.

ACKNOWLEDGMENTS

We thank M. Kliem and L. Newton for expert technical assistance.

GRANTS

This work was supported by National Institutes of Health Grants NS-054976, NS-042250, and RR-000165 to the Yerkes National Primate Research Center.

REFERENCES

Anderson JJ, Kuo S, Chase TN, Engber TM. GABAA and GABAB receptors differentially regulate striatal acetylcholine release in vivo. *Neurosci Lett* 160: 126–130, 1993.

Aosaki T, Kimura M, Graybiel AM. Temporal and spatial characteristics of tonically active neurons of the primate's striatum. *J Neurophysiol* 73: 1234–1252, 1995.

Aosaki T, Tsubokawa H, Ishida A, Watanabe K, Graybiel AM, Kimura M. Responses of tonically active neurons in the primate's striatum undergo systematic changes during behavioral sensorimotor conditioning. *J Neurosci* 14: 3969–3984, 1994.

Bauer R, Brosch M, Eckhorn R. Different rules of spatial summation from beyond the receptive field for spike rates and oscillation amplitudes in cat visual cortex. *Brain Res* 669: 291–297, 1995.

Bedard C, Kroger H, Destexhe A. Modeling extracellular field potentials and the frequency-filtering properties of extracellular space. *Biophys J* 86: 1829–1842, 2004.

Benedek K, Juhasz C, Muzik O, Chugani DC, Chugani HT. Metabolic changes of subcortical structures in intractable focal epilepsy. *Epilepsia* 45: 1100–1105, 2004.

Bennett BD, Wilson CJ. Synaptic regulation of action potential timing in neostriatal cholinergic interneurons. *J Neurosci* 18: 8539–8549, 1998.

Bennett BD, Wilson CJ. Spontaneous activity of neostriatal cholinergic interneurons in vitro. *J Neurosci* 19: 5586–5596, 1999.

Bevan MD, Booth PA, Eaton SA, Bolam JP. Selective innervation of neostriatal interneurons by a subclass of neuron in the globus pallidus of the rat. *J Neurosci* 18: 9438–9452, 1998.

Biraben A, Semah F, Ribeiro MJ, Douaud G, Remy P, Depaulis A. PET evidence for a role of the basal ganglia in patients with ring chromosome 20 epilepsy. *Neurology* 63: 73–77, 2004.

Bouilleret V, Semah F, Biraben A, Taussig D, Chassoux F, Syrota A, Ribeiro MJ. Involvement of the basal ganglia in refractory epilepsy: an 18F-fluoro-L-DOPA PET study using 2 methods of analysis. *J Nucl Med* 46: 540–547, 2005.

Bracci E, Centonze D, Bernardi G, Calabresi P. Voltage-dependent membrane potential oscillations of rat striatal fast-spiking interneurons. *J Physiol* 549: 121–130, 2003.

Bracci E, Centonze D, Bernardi G, Calabresi P. Engagement of rat striatal neurons by cortical epileptiform activity investigated with paired recordings. *J Neurophysiol* 92: 2725–2737, 2004.

Brown P, Williams D. Basal ganglia local field potential activity: character and functional significance in the human. *Clin Neurophysiol* 116: 2510–2519, 2005.

Calabresi P, Centonze D, Gubellini P, Pisani A, Bernardi G. Blockade of M2-like muscarinic receptors enhances long-term potentiation at corticostriatal synapses. *Eur J Neurosci* 10: 3020–3023, 1998.

Calabresi P, Centonze D, Gubellini P, Pisani A, Bernardi G. Acetylcholine-mediated modulation of striatal function. *Trends Neurosci* 23: 120–126, 2000.

Campbell K, Kalen P, Lundberg C, Wictorin K, Rosengren E, Bjorklund A. Extracellular gamma-aminobutyric acid levels in the rat caudate-putamen: monitoring the neuronal and glial contribution by intracerebral microdialysis. *Brain Res* 614: 241–250, 1993.

Charara A, Heilman TC, Levey AI, Smith Y. Pre- and postsynaptic localization of GABA(B) receptors in the basal ganglia in monkeys. *Neuroscience* 95: 127–140, 2000.

Collins DR, Pelletier JG, Paré D. Slow and fast (gamma) neuronal oscillations in the perirhinal cortex and lateral amygdala. *J Neurophysiol* 85: 1661–1672, 2001.

Courtemanche R, Pellerin JP, Lamarre Y. Local field potential oscillations in primate cerebellar cortex: modulation during active and passive expectancy. *J Neurophysiol* 88: 771–782, 2002.

Cowan RL, Wilson CJ, Emson PC, Heizmann CW. Parvalbumin-containing GABAergic interneurons in the rat neostriatum. *J Comp Neurol* 302: 197–205, 1990.

Cragg SJ. Meaningful silences: how dopamine listens to the ACh pause. *Trends Neurosci* 29: 125–131, 2006.

Crossman AR, Mitchell IJ, Sambrook MA, Jackson A. Chorea and myoclonus in the monkey induced by gamma-aminobutyric acid antagonism in the lentiform complex. The site of drug action and a hypothesis for the neural mechanisms of chorea. *Brain* 111: 1211–1233, 1988.

Czubayko U, Plenz D. Fast synaptic transmission between striatal spiny projection neurons. *Proc Natl Acad Sci USA* 99: 15764–15769, 2002.

Darbin O, Newton L, Wichmann T. A new probe to monitor the effects of drugs on local field potentials. *J Neurosci Methods* 155: 291–295, 2006.

Darbin O, Risso JJ, Rostain JC. High pressure enhanced NMDA activity in the striatum and the globus pallidus: relationships with myoclonia and locomotor and motor activity in rat. *Brain Res* 852: 62–67, 2000.

DeBoer P, Westerink BH. GABAergic modulation of striatal cholinergic interneurons: an in vivo microdialysis study. *J Neurochem* 62: 70–75, 1994.

DeLong MR, Wichmann T. Circuits and circuit disorders of the basal ganglia. *Arch Neurol* 64: 20–24, 2007.

Dematteis M, Kahane P, Vercueil L, Depaulis A. MRI evidence for the involvement of basal ganglia in epileptic seizures: an hypothesis. *Epileptic Disord* 5: 161–164, 2003.

Djurfeldt M, Ekeberg O, Graybiel AM. Cortex-basal ganglia interaction and attractor states. *Neurocomputing* 38–40: 573–579, 2001.

Donoghue JP, Sanes JN, Hatsopoulos NG, Gaal G. Neural discharge and local field potential oscillations in primate motor cortex during voluntary movements. *J Neurophysiol* 79: 159–173, 1998.

Frank MJ, Claus ED. Anatomy of a decision: striato-orbitofrontal interactions in reinforcement learning, decision making, and reversal. *Psychol Rev* 113: 300–326, 2006.

Fredow G, Loscher W. Effects of pharmacological manipulation of GABAergic neurotransmission in a new mutant hamster model of paroxysmal dystonia. *Eur J Pharmacol* 192: 207–219, 1991.

Fujiyama F, Fritschy JM, Stephenson FA, Bolam JP. Synaptic localization of GABA(A) receptor subunits in the striatum of the rat. *J Comp Neurol* 416: 158–172, 2000.

Galvan VV, Chen J, Weinberger NM. Differential thresholds of local field potentials and unit discharges in rat auditory cortex. *Hear Res* 167: 57–60, 2002.

Goldberg JA, Rokni U, Boraud T, Vaadia E, Bergman H. Spike synchronization in the cortex/basal-ganglia networks of parkinsonian primates reflects global dynamics of the local field potentials. *J Neurosci* 24: 6003–6010, 2004.

Graybiel AM. The basal ganglia: learning new tricks and loving it. *Curr Opin Neurobiol* 15: 638–644, 2005.

Gustafson N, Gireesh-Dharmaraj E, Czubayko U, Blackwell KT, Plenz D. A comparative voltage- and current-clamp analysis of feedback and feedforward synaptic transmission in the striatal microcircuit in vitro. *J Neurophysiol* 95: 737–752, 2006.

Hellgren Kotaleski J, Plenz D, Blackwell KT. Using potassium currents to solve signal to noise problems in inhibitory feedforward networks of the striatum. *J Neurophysiol* 95: 331–341, 2006.

Hernandez-Echeagaray E, Galarraga E, Bargas J. 3-Alpha-chloro-imperialine, a potent blocker of cholinergic presynaptic modulation of glutamatergic afferents in the rat neostriatum. *Neuropharmacology* 37: 1493–1502, 1998.

Hikosaka O, Nakamura K, Sakai K, Nakahara H. Central mechanisms of motor skill learning. *Curr Opin Neurobiol* 12: 217–222, 2002.

Hu XT, Wang RY. Comparison of effects of D-1 and D-2 dopamine receptor agonists on neurons in the rat caudate putamen: an electrophysiological study. *J Neurosci* 8: 4340–4348, 1988.

Institute for Laboratory Animal Research/Office of Laboratory Animal Welfare (ILAC/OLAW) of the National Institutes of Health. *Guide for the Care and Use of Laboratory Animals* (7th ed.). Washington, DC: National Research Council/National Academy Press, 1996.

Jaeger D, Gilman S, Aldridge JW. Neuronal activity in the striatum and pallidum of primates related to the execution of externally cued reaching movements. *Brain Res* 694: 111–127, 1995.

Jaeger D, Kita H, Wilson CJ. Surround inhibition among projection neurons is weak or nonexistent in the rat neostriatum. *J Neurophysiol* 72: 2555–2558, 1994.

Kaneda K, Kita H. Synaptically released GABA activates both pre- and postsynaptic GABA(B) receptors in the rat globus pallidus. *J Neurophysiol* 94: 1104–1114, 2005.

Kaur S, Lazar R, Metherate R. Intracortical pathways determine breadth of subthreshold frequency receptive fields in primary auditory cortex. *J Neurophysiol* 91: 2551–2567, 2004.

Kawaguchi Y. Physiological, morphological, and histochemical characterization of three classes of interneurons in rat neostriatum. *J Neurosci* 13: 4908–4923, 1993.

Kawaguchi Y, Wilson CJ, Augood SJ, Emson PC. Striatal interneurones: chemical, physiological and morphological characterization. *Trends Neurosci* 18: 527–535, 1995.

Kemp JM, Powell TPS. The cortico-striate projection in the monkey. *Brain* 93: 525–546, 1970.

Kita H. GABAergic circuits of the striatum. *Prog Brain Res* 99: 51–72, 1993.

Kita H. Glutamatergic and GABAergic postsynaptic responses of striatal spiny neurons to intrastriatal and cortical stimulation recorded in slice preparations. *Neuroscience* 70: 925–940, 1996.

Kita H. Globus pallidus external segment. *Prog Brain Res* 160: 111–133, 2007.

Koos T, Tepper JM. Inhibitory control of neostriatal projection neurons by GABAergic interneurons. *Nat Neurosci* 2: 467–472, 1999.

Koos T, Tepper JM. Dual cholinergic control of fast-spiking interneurons in the neostriatum. *J Neurosci* 22: 529–535, 2002.

Koos T, Tepper JM, Wilson CJ. Comparison of IPSCs evoked by spiny and fast-spiking neurons in the neostriatum. *J Neurosci* 24: 7916–7922, 2004.

Kreil A, Richter A. Antidystonic efficacy of gamma-aminobutyric acid uptake inhibitors in the dtsz mutant. *Eur J Pharmacol* 521: 95–98, 2005.

Lacey CJ, Boyes J, Gerlach O, Chen L, Magill PJ, Bolam JP. $GABA_B$ receptors at glutamatergic synapses in the rat striatum. *Neuroscience* 136: 1083–1095, 2005.

Lapper SR, Bolam JP. Input from the frontalcortex and the parafascicular nucleus to cholinergic interneurons in the dorsal striatum of the rat. *Neuroscience* 51: 533–545, 1992.

Laubach M. Who's on first? What's on second? The time course of learning in corticostriatal systems. *Trends Neurosci* 28: 509–511, 2005.

Loopuijt LD, van der Kooy D. Organization of the striatum: collateralization of its efferent axons. *Brain Res* 348: 86–99, 1985.

Loscher W, Horstermann D. Abnormalities in amino acid neurotransmitters in discrete brain regions of genetically dystonic hamsters. *J Neurochem* 59: 689–694, 1992.

Malenka RC, Kocsis JD. Presynaptic actions of carbachol and adenosine on corticostriatal synaptic transmission studied in vitro. *J Neurosci* 8: 3750–3756, 1988.

Mallet N, Ballion B, Le Moine C, Gonon F. Cortical inputs and GABA interneurons imbalance projection neurons in the striatum of parkinsonian rats. *J Neurosci* 26: 3875–3884, 2006.

Mallet N, Le Moine C, Charpier S, Gonon F. Feedforward inhibition of projection neurons by fast-spiking GABA interneurons in the rat striatum in vivo. *J Neurosci* 25: 3857–3869, 2005.

Marsden CD, Meldrum BS, Pycock C, Tarsy D. Focal myoclonus produced by injection of picrotoxin into the caudate nucleus of the rat (Abstract). *J Physiol* 246: 96P, 1975.

Martone ME, Armstrong DM, Young SJ, Groves PM. Ultrastructural examination of enkephalin and substance P input to cholinergic neurons within the rat neostriatum. *Brain Res* 594: 253–262, 1992.

Matsumoto N, Minamimoto T, Graybiel AM, Kimura M. Neurons in the thalamic CM-Pf complex supply striatal neurons with information about behaviorally significant sensory events. *J Neurophysiol* 85: 960–976, 2001.

Meredith GE, Wouterlood FG. Hippocampal and midline thalamic fibers and terminals in relation to the choline acetyltransferase-immunoreactive neurons in nucleus accumbens of the rat: a light and electron microscopic study. *J Comp Neurol* 296: 204–221, 1990.

Morris G, Arkadir D, Nevet A, Vaadia E, Bergman H. Coincident but distinct messages of midbrain dopamine and striatal tonically active neurons. *Neuron* 43: 133–143, 2004.

Nakamura S, Muramatsu S, Yoshida M. Role of the basal ganglia in manifestation of rhythmical jaw movement in rats. *Brain Res* 535: 335–338, 1990.

Nicola SM, Woodward Hopf F, Hjelmstad GO. Contrast enhancement: a physiological effect of striatal dopamine? *Cell Tissue Res* 318: 93–106, 2004.

Nisenbaum ES, Berger TW, Grace AA. Presynaptic modulation by GABAB receptors of glutamatergic excitation and GABAergic inhibition of neostriatal neurons. *J Neurophysiol* 67: 477–481, 1992.

Nobrega JN, Richter A, Burnham WM, Loscher W. Alterations in the brain GABAA/benzodiazepine receptor-chloride ionophore complex in a genetic model of paroxysmal dystonia: a quantitative autoradiographic analysis. *Neuroscience* 64: 229–239, 1995.

Norena A, Eggermont JJ. Comparison between local field potentials and unit cluster activity in primary auditory cortex and anterior auditory field in the cat. *Hear Res* 166: 202–213, 2002.

Ouyang C, Guo L, Lu Q, Xu X, Wang H. Enhanced activity of GABA receptors inhibits glutamate release induced by focal cerebral ischemia in rat striatum. *Neurosci Lett* 420: 174–178, 2007.

Pakhotin P, Bracci E. Cholinergic interneurons control the excitatory input to the striatum. *J Neurosci* 27: 391–400, 2007.

Parent M, Parent A. Single-axon tracing study of corticostriatal projections arising from primary motor cortex in primates. *J Comp Neurol* 496: 202–213, 2006.

Parthasarathy HB, Graybiel AM. Cortically driven immediate-early gene expression reflects modular influence of sensorimotor cortex on identified striatal neurons in the squirrel monkey. *J Neurosci* 17: 2477–2491, 1997.

Perez-Rosello T, Figueroa A, Salgado H, Vilchis C, Tecuapetla F, Guzman JN, Galarraga E, Bargas J. Cholinergic control of firing pattern and neurotransmission in rat neostriatal projection neurons: role of CaV2.1 and CaV2.2 Ca^{2+} channels. *J Neurophysiol* 93: 2507–2519, 2005.

Pisani A, Bernardi G, Ding J, Surmeier DJ. Re-emergence of striatal cholinergic interneurons in movement disorders. *Trends Neurosci* 30: 545–553, 2007.

Plenz D, Kitai ST. Up and down states in striatal medium spiny neurons simultaneously recorded with spontaneous activity in fast-spiking interneurons studied in cortex-striatum-substantia nigra organotypic cultures. *J Neurosci* 18: 266–283, 1998.

Pratt GD, Richter A, Mohler H, Loscher W. Regionally selective and age-dependent alterations in benzodiazepine receptor binding in the genetically dystonic hamster. *J Neurochem* 64: 2153–2158, 1995.

Raz A, Feingold A, Zelanskaya V, Vaadia E, Bergman H. Neuronal synchronization of tonically active neurons in the striatum of normal and parkinsonian primates. *J Neurophysiol* 76: 2083–2088, 1996.

Richter A, Loscher W. Alterations in pharmacological sensitivity of GABAergic but not dopaminergic and glutamatergic systems during ontogenesis in dystonic mutant hamsters. *Eur J Pharmacol* 231: 111–119, 1993.

Riedel A, Hartig W, Fritschy JM, Bruckner G, Seifert U, Brauer K. Comparison of the rat dorsal and ventral striatopallidal system. A study using the GABA(A)-receptor alpha1-subunit and parvalbumin immunolabeling. *Exp Brain Res* 121: 215–221, 1998.

Rymar VV, Sasseville R, Luk KC, Sadikot AF. Neurogenesis and stereological morphometry of calretinin-immunoreactive GABAergic interneurons of the neostriatum. *J Comp Neurol* 469: 325–339, 2004.

Sadek AR, Magill PJ, Bolam JP. A single-cell analysis of intrinsic connectivity in the rat globus pallidus. *J Neurosci* 27: 6352–6362, 2007.

Sandstrom MI, Rebec GV. Characterization of striatal activity in conscious rats: contribution of NMDA and AMPA/kainate receptors to both spontaneous and glutamate-driven firing. *Synapse* 47: 91–100, 2003.

Sasaki M, Matsuda H, Omura I, Sugai K, Hashimoto T. Transient seizure disappearance due to bilateral striatal necrosis in a patient with intractable epilepsy. *Brain Dev* 22: 50–55, 2000.

Sato F, Lavallee P, Levesque M, Parent A. Single-axon tracing study of neurons of the external segment of the globus pallidus in primate. *J Comp Neurol* 417: 17–31, 2000.

Schultz W, Tremblay L, Hollerman JR. Changes in behavior-related neuronal activity in the striatum during learning. *Trends Neurosci* 26: 321–328, 2003.

Sidibé M, Smith Y. Thalamic inputs to striatal interneurons in monkeys: synaptic organization and co-localization of calcium binding proteins. *Neuroscience* 89: 1189–1208, 1999.

Siegel JM. Brainstem mechanisms generating REM sleep. In: *Principles and Practice of Sleep Medicine*, edited by Kryger MH, Roth T, Dement WC. Philadelphia, PA: Saunders, 1989, p. 104–120.

Slaght SJ, Paz T, Chavez M, Deniau JM, Mahon S, Charpier S. On the activity of the corticostriatal networks during spike-and-wave discharges in a genetic model of absence epilepsy. *J Neurosci* 24: 6816–6825, 2004.

Smith Y, Parent A. Differential connections of caudate nucleus and putamen in the squirrel monkey (Saimiri sciureus). *Neuroscience* 18: 347–371, 1986.

Smith Y, Raju DV, Paré J-F, Sidibé M. The thalamostriatal system: a highly specific network of the basal ganglia circuitry. *Trends Neurosci* 27: 520–527, 2004.

Soares J, Kliem MA, Betarbet R, Greenamyre JT, Yamamoto B, Wichmann T. Role of external pallidal segment in primate parkinsonism: comparison of the effects of MPTP-induced parkinsonism and lesions of the external pallidal segment. *J Neurosci* 24: 6417–6426, 2004.

Stern EA, Jaeger D, Wilson CJ. Membrane potential synchrony of simultaneously recorded striatal spiny neurons in vivo. *Nature* 394: 475–478, 1998.

Sugita S, Uchimura N, Jiang ZG, North RA. Distinct muscarinic receptors inhibit release of gamma-aminobutyric acid and excitatory amino acids in mammalian brain. *Proc Natl Acad Sci USA* 88: 2608–2611, 1991.

Takahashi H, Straschill M. The effects of focal epileptic activity on the somatosensory evoked potentials in the rat. *Arch Psychiatr Nervenkr* 231: 81–91, 1981.

Taverna S, van Dongen YC, Groenewegen HJ, Pennartz CM. Direct physiological evidence for synaptic connectivity between medium-sized spiny neurons in rat nucleus accumbens in situ. *J Neurophysiol* 91: 1111–1121, 2004.

Tecuapetla F, Carrillo-Reid L, Guzman JN, Galarraga E, Bargas J. Different inhibitory inputs onto neostriatal projection neurons as revealed by field stimulation. *J Neurophysiol* 93: 1119–1126, 2005.

Tepper JM, Bolam JP. Functional diversity and specificity of neostriatal interneurons. *Curr Opin Neurobiol* 14: 685–692, 2004.

Tepper JM, Koos T, Wilson CJ. GABAergic microcircuits in the neostriatum. *Trends Neurosci* 27: 662–669, 2004.

Tunstall MJ, Oorschot DE, Kean A, Wickens JR. Inhibitory interactions between spiny projection neurons in the rat striatum. *J Neurophysiol* 88: 1263–1269, 2002.

Venance L, Glowinski J, Giaume C. Electrical and chemical transmission between striatal GABAergic output neurones in rat brain slices. *J Physiol* 559: 215–230, 2004.

Vercueil L, Kahane P, Francois-Joubert A, Hirsch E, Hoffmann D, Depaulis A, Marescaux C. Basal ganglia involvement in rotational seizures. *Epileptic Disord* 1: 107–112, 1999.

Waldvogel HJ, Billinton A, White JH, Emson PC, Faull RL. Comparative cellular distribution of GABAA and GABAB receptors in the human basal ganglia: immunohistochemical colocalization of the alpha 1 subunit of the GABAA receptor, and the GABABR1 and GABABR2 receptor subunits. *J Comp Neurol* 470: 339–356, 2004.

Westerink BH, De Vries JB. A method to evaluate the diffusion rate of drugs from a microdialysis probe through brain tissue. *J Neurosci Methods* 109: 53–58, 2001.

Wu Y, Parent A. Striatal interneurons expressing calretinin, parvalbumin or NADPH-diaphorase: a comparative study in the rat, monkey and human. *Brain Res* 863: 182–191, 2000.

Yoshida M, Nagatsuka Y, Muramatsu S, Niijima K. Differential roles of the caudate nucleus and putamen in motor behavior of the cat as investigated by local injection of GABA antagonists. *Neurosci Res* 10: 34–51, 1991.

Zackheim J, Abercrombie ED. Thalamic regulation of striatal acetylcholine efflux is both direct and indirect and qualitatively altered in the dopamine-depleted striatum. *Neuroscience* 131: 423–436, 2005.